Effects of annealing on luminescence efficiency of large-size YAG:Ce crystal grown by temperature gradient techniques

Dunhua Cao (曹顿华)[1,2], **Guangjun Zhao (赵广军)**[1*], **Qin Dong (董 勤)**[1,2], **Jianyu Chen (陈建玉)**[1,2],

Yan Cheng (程 艳)[1,2], **Yuchong Ding (丁雨憧)**[1,2], **and Jun Zou (邹 军)**[3,4]

[1]*Key Laboratory of Material Science and Technology for High Power Lasers,*

Shanghai Institute of Optics and Fine Mechanics, Shanghai 201800, China

[2]*Graduate University of the Chinese Academy of Science, Beijing 100049, China*

[3]*Zhejiang Gemcore Technology Co., Ltd, Wenzhou 325035, China*

[4]*Wenzhou University, Wenzhou 325035, China*

E-mail: zhaoguangjun@163.net

Received April 15, 2009

YAG:Ce crystal with a diameter of 110 mm is successfully grown by the temperature gradient technique (TGT). The effects of annealing on the luminescence efficiency of YAG:Ce crystal are investigated, and the optimal annealing temperature and atmosphere are obtained. The mechanism of variation behavior of the luminescence efficiency of YAG:Ce under different annealing conditions is discussed and some details on the luminescence associated with color centers are analyzed.

OCIS codes: 160.5690, 300.1030, 300.2140, 300.6560.

doi: 10.3788/COL20100802.0199.

Ce^{3+} doped yttrium-aluminum garnet (YAG:Ce) is a well established scintillator and has many attractive properties, such as fast decay (60–100 ns), high light yield (about 20000 photons/MeV), emission peaks at 520–550 nm that well match with the sensitivity of commercial Si-based charge-coupled device (CCD) detectors, and good mechanical and chemical stability[1−4]. These properties have made YAG:Ce a material for many applications, including CCD detectors, high count-rate devices, detection of light charged particles, white light emitting diode (LED), and gamma ray detection[4−7].

It is quite important to grow large-size YAG:Ce scintillators with high quality for scintillation applications. At present, YAG:Ce scintillation crystals are grown mainly by Czochralski (Cz) methods, which have some disadvantages compared with temperature gradient techniques (TGT). Firstly, TGT method can avoid the cores at the center of the crystals which will be easily formed during Cz growth and the cores are very deleterious to the optical homogeneity of the crystals[8]. Secondly, TGT method helps to incorporate a large amount of Ce ions into the lattice, because of constitutional super-cooling effect and second-phase precipitation. In addition, it is much easier to get large-size crystals by TGT[9]. The other important factor affecting the scintillation application of YAG:Ce crystals is annealing[10]. However, the mechanism of the annealing and the optimum annealing temperature and atmosphere are still unknown yet.

In this letter, YAG:Ce crystal with a diameter of 110 mm was grown by TGT method. The effects of heat-treatment processes on the luminescence efficiency of the YAG:Ce crystal were investigated and the optimal annealing temperature and atmosphere were provided, which helped to improve the light yields of YAG:Ce scintillator crystals grown by TGT. The mechanism of variation behavior of the luminescence efficiency of YAG:Ce was discussed and some details on the spectroscopic char-

acteristics associated with color centers were presented.

The YAG:Ce crystal was grown by TGT under strong reducing atmosphere produced by the graphite heating element. The highly pure oxide powders Y_2O_3 (5N), CeO_2 (5N), and Al_2O_3 (5N) were used and the final chemical formula is $(Y_{0.997}Ce_{0.003})_3Al_5O_{12}$. The seed was <111> orientation and the whole growth atmosphere was high-purity Ar gas. More details of the growth process can be found in Ref. [9].

The color of the as-grow crystal became yellow by annealing in air or hydrogen atmosphere and became black due to the volatile carbon entering into the crystal from the heater during the growth. Figure 1 shows the picture of the as-grown YAG:Ce crystal with size of $\Phi110\times 50$ (mm).

The spectroscopic samples were optically polished to planets with dimensions of $15\times10\times2$ (mm). The luminescence spectra of the samples were measured by the fluorescence spectrometer (FP-6500, JASCO, Japan). The transmission spectra were taken with the UV/VIS spectrophotometer (V-570, JASCO, Japan). The X-ray excited luminessence (XEL) spectra were measured by
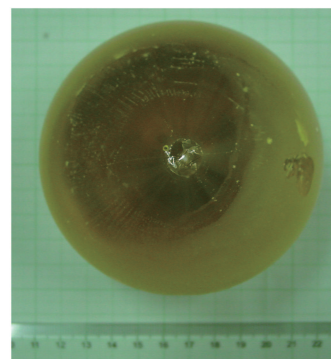

Fig. 1. As-grown YAG:Ce crystal grown by TGT.

an X-ray excited spectrometer, a grating monochromator (SBP, Zolix, China) and a photomultiplier tube (CR131, Hamamatsu, Japan) under the same condition (35 kV, 20 mA) at room temperature.

Considering the positive effects of annealing on improving the spectral properties of the YAG:Ce crystals grown by TGT, we annealed the YAG:Ce samples in different temperatures and atmospheres to get the optimum annealing condition. Absorption spectra of the YAG:Ce samples annealed in different atmospheres are shown in Fig. 2. The absorption peaks at 228, 340 and 458 nm are observed in all of the samples, which can be attributed to the 4f→5d interconfigurational absorption of Ce^{3+} ions in YAG:Ce crystal. Two additional bands centered at 300 and 371 nm are also observed, which have been ascribed to color centers[5]. It was found that these two peaks decreased after annealing in H_2 atmosphere at 1100 °C, and vanished after annealing in air and reducing atmosphere above 1100 °C for 10 hours. Generally the oxygen vacancies in the crystals will increase when the crystal is annealed in H_2 atmosphere, which reveals that the absorption peaks at 300 and 371 nm are not caused by oxygen vacancies. The absorption of the as-grown YAG:Ce crystal in the 240 and 420 nm ranges is very strong as well as that of the sample annealed in H_2 atmosphere at 1100 °C, which may be caused by carbon volatiles from the heater during growth.

Figure 3 presents the emission spectra of the YAG:Ce samples under different annealing conditions. The Ce^{3+} luminescence bands of the YAG:Ce samples under 458 nm excitation before and after annealing are all peaked at 525 nm, but their emission intensity varies significantly. Figure 4 shows that the emission intensity of the samples enhances remarkably in the air-annealing atmosphere with the strongest emission intensity at 1100 °C, and then reduces with increase of the annealing temperature. The emission intensity varies in the opposite trend in the H_2 atmosphere with the lowest emission intensity at 1100 °C. The luminescence intensity of the sample annealed in the air atmosphere at 1100 °C is nearly 60% higher than that of the as-grown sample.

Figure 5 presents the XEL spectra of the YAG:Ce crystals annealed under different conditions. The emission bands at 525 nm of YAG:Ce are similar to those under 458-nm excitation (Fig. 3), but the strong new emissions at 300 and 354 nm appear in all of the samples, and an additional band peaked at 391 nm is observed in the emission spectra of the as-grown sample.
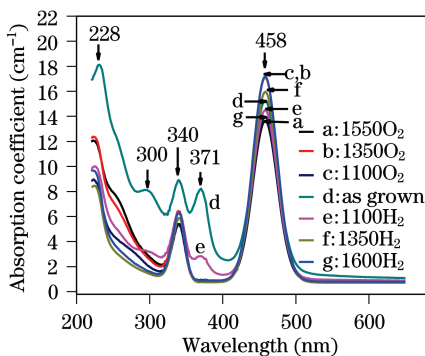

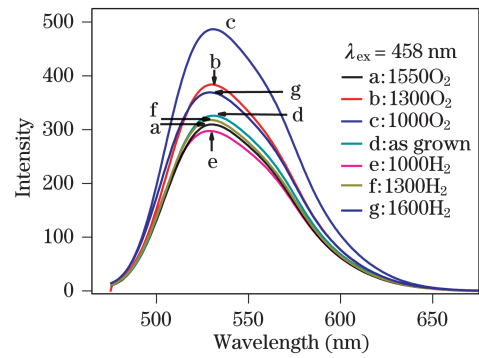Fig. 2. Absorption spectra of YAG:Ce annealed in different atmosphere.

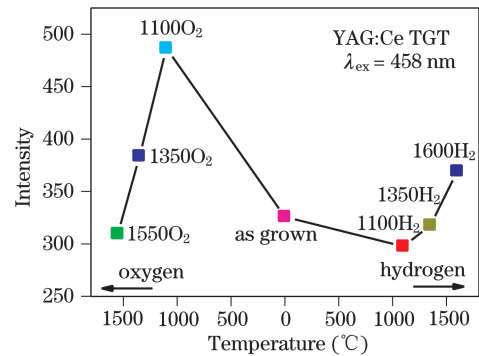Fig. 3. Emission spectra of YAG:Ce annealed in different atmosphere.

Fig. 4. Variation behaviors of the emission intensity of YAG:Ce annealed in different atmosphere.

Recalling that the absorption bands at 300 and 371 nm of the as-grown YAG:Ce vanish after annealed in both air and reducing atmospheres above 1100 °C (Fig. 2), we suppose that color centers probably formed by carbon-related complex defects during the growth, and after annealing the carbon volatilize, and the emission bands disappear. The 300-nm emission band of the crystals has been attributed to the Y_{Al} anti-site defects (ADs) (Y cations localized in octahedral sites of the Al cations) and the self-trapped excitons (STEs)[11,12].

The variation behavior of the XEL emission intensity of YAG:Ce annealed under different conditions (Fig. 6) is similar to those under 458-nm excitation (Fig. 4). Since the photons emitted from the inner of the samples will be re-absorbed due to high absorption, the XEL emission intensities of the as-grown YAG:Ce at 300, 354 and 525 nm are relative low, which can be improved by annealing. Since the crystal was grown in a reducing atmosphere by TGT, there may be relatively more Ce^{2+} ions in the as-grown crystal. These Ce^{2+} ions are not stable and will transfer into Ce^{3+} ions and enhance the intensity of emission band at 525 nm after annealing in air atmosphere. However, with the increase of the annealing temperature, Ce^{3+} ions can easily lose an electron and become Ce^{4+} ions[13], which will result in the quenching of Ce^{3+} emission[14].

The XEL spectra taken after the reducing annealing show increase of emission intensity with the strongest at 1350 °C, which is mainly caused by the vanishing of defects associated with carbon and the valence-state change of Ce ions. Other complex defects such as oxygen vacancies, ADs, and cation vacancies are also the
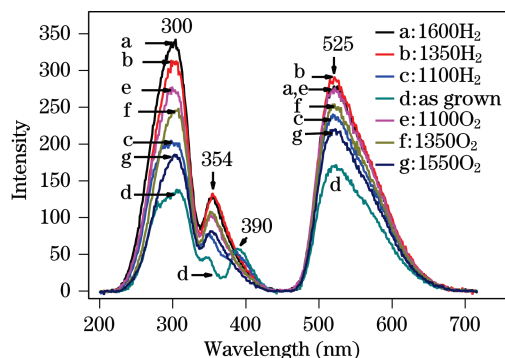
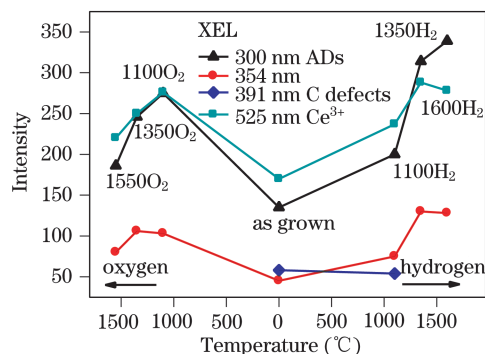Fig. 5. XEL spectra of YAG:Ce annealed in different atmosphere.

Fig. 6. Variation behaviors of XEL intensity of YAG:Ce annealed in different atmosphere.

reasons that may affect the luminescence efficiency of YAG:Ce in the process of annealing[15]. Comparing the luminescence efficiency of samples annealed under different conditions and the cost of heating treatment, we concluded that the air annealing at 1100 °C was the optimal annealing condition.

In conclusion, the YAG:Ce crystal with a diameter of 110 mm is grown by TGT successfully. The effects of heat-treatment processes on the luminescence efficiency of YAG:Ce crystal are investigated, and the results show that air annealing at 1100 °C is the optimum annealing condition for YAG:Ce (TGT), which will help to improve the light yields of YAG:Ce. The mechanism of the variation behavior of the luminescence efficiency of YAG:Ce (TGT) is discussed. The study reveals that the absorption bands at 300 and 371 nm of the as-grown YAG:Ce

are not caused by oxygen vacancies, and we suppose that the color centers are probably due to complex defects associated with carbon formed during the growth.

References

1. T. Ludziejewski, M. Moszyński, M. Kapusta, D. Wolski, W. Klamra, and K. Moszyńska, Nucl. Instrum. Meth. Phys. Res. A **398,** 287 (1997).
2. S. Baccaro, K. Blažek, F. de Notaristefani, P. Maly, J. A. Mares, R. Pani, R. Pellegrini, and A. Soluri, Nucl. Instrum. Meth. Phys. Res. A **361,** 209 (1995).
3. X. He, G. Zhao, X. Xun, X. Zeng, and J. Xu, Chin. Opt. Lett. **5,** 295 (2007).
4. I. Daberkow, K. H. Herrmann, L. Liu, W. D. Rau, and H. Tietz, Ultramicroscopy **64,** 35 (1996).
5. T. Bhattacharjee, S. K. Basu, C. C. Dey, and M. B. Chatterjee, Nucl. Instrum. Meth. Phys. Res. A **484,** 364 (2002).
6. L. Ye, L. Song, and G. Lin, Acta Opt. Sin. (in Chinese) **29,** (Suppl. 1) 169 (2009).
7. T. Yanagida, T. Itoh, H. Takahashi, S. Hirakuri, M. Kokubun, K. Makishima, M. Sato, T. Enoto, T. Yanagitani, H. Yagi, T. Shigetad, and T. Ito, Nucl. Instrum. Meth. Phys. Res. A **579,** 23 (2007).
8. P. Yang, P. Deng, Z. Yin, and Y. Tian, J. Crystal Growth **218,** 87 (2000).
9. G. Zhao, X. Zeng, J. Xu, Y. Xu, and Y. Zhou, J. Crystal Growth **253,** 290 (2003).
10. X. Zeng, G. Zhao, J. Xu, H. Li, X. He, H. Pang, and M. Jie, J. Crystal Growth **274,** 495 (2005).
11. Y. Zorenko, V. Gorbenko, I. Konstankevych, B. Girinev, and M. Globus, Nucl. Instrum. Meth. Phys. Res. A **486,** 309 (2002).
12. Y. Zorenko, A. Voloshinovskii, I. Konstankevych, V. Kolobanov, V. Mikhailin, and D. Spassky, Radiat. Meas. **38,** 677 (2004).
13. S. R. Rotman, H. L. Tuller, and C. Warde, J. Appl. Phys. **71,** 1209 (1992).
14. G. Özen and B. Demirata, Spectrochim. Acta Mol. Biomol. Spectros. **56,** 1795 (2000).
15. F. A. Selim, D. Solodovnikov, M. H. Weber, and K. G. Lynn, Appl. Phys. Lett. **91,** 104105 (2007).